Automatic Design of PM Motor Using Monte Carlo Tree Search in Conjunction with Topology Optimization

Hayaho Sato[1] and Hajime Igarashi[1]

[1]Graduate School of Information Science and Technology, Hokkaido University, Sapporo, 060-0814, Japan

A novel automatic design method for permanent magnet (PM) motors using a Monte Carlo tree search is presented. The optimal motor structures are determined through a tree search in which the motors with different numbers of poles, current phase angles, PM configurations, and numbers of PMs are simultaneously considered. At the leaf nodes, parameter and topology optimizations are performed to obtain the optimal material shape and distribution. The proposed method was applied to the optimization of a 24-slot motor. It was shown to be effective in finding the optimal motor structure and geometry to maximize the average torque while considering iron loss. The proposed method can be applied not only to the design of PM motors but also to many types of electric apparatus and other systems.

Index Terms—**Design optimization, Permanent magnet motors, Tree data structures**

I. Introduction

THE DEMAND for high-performance permanent magnet (PM) motors has been increasing. For the design of PM motors, shape optimization based on electromagnetic analysis and stochastic optimization algorithms plays an important role. Parameter optimization (PO) and topology optimization (TO) are used for this purpose. The shape parameters, such as length and position, which must be set beforehand, are determined in PO, which leads to a manufacturable structure. The material distribution in the design region is determined by TO, accepting the generation and annihilation of holes without introducing shape parameters [1], [2]. Owing to its properties, TO can generate novel shapes without human dependency. It has been shown that PO and TO can be performed simultaneously to leverage their advantages [3]. This is called here "hybridized parameter–topology optimization" (PTO). For the design of PM motors, it would be effective to determine the position and shape of the PM by PO for ease of manufacturing, whereas determining the magnetic core shape by TO with high flexibility would be appropriate.

There are still limitations for these approaches. One must assume basic structures of PM motors, such as the number of poles and PM configurations before optimization, which have considerable effects on their design. To realize automatic design that determines not only the machine shape but also basic machine structures, a method that combines tree search and reinforcement learning has been proposed [4]. This method associates basic machine parameters with tree nodes. The machine structures are selected and evaluated based on exploration and exploitation. Although the method has been shown to be effective for the design of linear induction motors, it would be difficult to find a novel structure because it is based on PO. Moreover, the automatic design of PM motors is not considered.

In this article, a novel automatic design method for PM motors is proposed based on a Monte Carlo tree search (MCTS), which has been used for generic gaming artificial intelligence (AI) [5] and field computations [6]. In the proposed method, the basic structure of PM motors is determined by MCTS performing PTO to obtain a novel rotor structure at the leaf of the tree. The method is applied to the optimization of the PM motor to maximize the average torque under given constraints. It was compared with the conventional PTO, where the basic structure was predetermined.

Manuscript received April 1, 2015; revised May 15, 2015; Corresponding author: H. Sato (e-mail: hayaho_sato@em.ist.hokudai.ac.jp).

Color versions of one or more of the figures in this paper are available online at http://ieeexplore.ieee.org.

Digital Object Identifier (inserted by IEEE).

II. Automatic Design Method

A. Problem definition

The optimal design problem is given by

$$F(\boldsymbol{s},\boldsymbol{r}) \to \max., \tag{1a}$$

$$\text{sub. to } G_i(\boldsymbol{s},\boldsymbol{r}) \geq 0 \ (i = 1,\dots,n_\mathrm{c}), \tag{1b}$$

where F and G_i are the objective and constraint functions, respectively, and n_c is the number of constraints. The parameter $\boldsymbol{s}$ represents the basic motor structure, such as the number of poles, while $\boldsymbol{r}$ represents the rotor geometry defining the position and shape of the PMs, as well as the rotor shape. The goal is to optimize $\boldsymbol{s},\boldsymbol{r}$ to maximize $F(\boldsymbol{s},\boldsymbol{r})$ under the given constraints.

B. Automatic design method

The algorithm of the proposed method is schematically shown in Fig. 1. The basic machine parameters are associated with the tree nodes. Once a path from the root to the leaf node is determined, the basic motor structure parameterized by $\boldsymbol{s}$ is defined. For $\boldsymbol{s}$, the number of poles P_n, current phase angle β, PM configuration, and number of PMs are considered.

When n_i, v_i are the number of visits and the value for node i, the value v_i is defined as the average of $F(\boldsymbol{s},\boldsymbol{r})$ obtained during the tree search iterations. The algorithm is summarized as follows.

1. Set $n_i \leftarrow 0$, $v_i \leftarrow 0$ for all nodes. Set number of iterations $t \leftarrow 0$.
2. *Selection*: Select a node, which corresponds to a basic parameter, to visit. Under parent node p, node i with

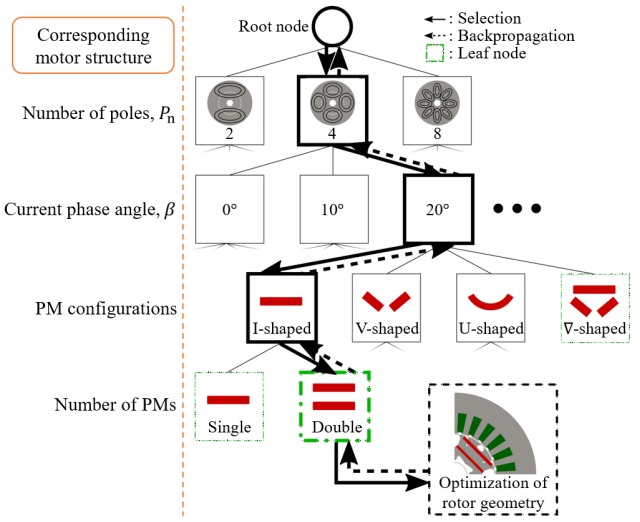

Fig. 1. Proposed automatic design method. Current phase angle is selected from {0, 10, 20, 30, 40}.

the largest value of $P(p,i)$ defined by

$$P(p,i) = v_i + C\sqrt{(\ln n_p)/n_i}, \tag{2}$$

is selected [7], where C is a constant that controls the balance between exploration and exploitation. As C becomes larger, greater focus is placed on exploration. In this study, C is set to 0.5. If $n_i = 0$, $P(p,i)$ is set to a sufficiently large value.

This operation starts from the root node and is repeated until one of the leaf nodes is reached. Here, $\boldsymbol{s}$ is determined from the selection result.

3. *Optimization:* After selection, PTO (described later) is performed to maximize $F(\boldsymbol{s},\boldsymbol{r})$ to obtain the optimal rotor geometry parameter $\boldsymbol{r}$ under given $\boldsymbol{s}$. Here, a motor model with optimal rotor geometry is obtained, which has the value F_t of the objective function.
4. *Backpropagation:* Update n_i and v_i for all visited nodes. The value v_i is defined as

$$v_i = \frac{1}{n_i}\sum_{j=1}^{n_i} F_j, \tag{3}$$

where j is the internal index over visits in node i.

5. If t reaches a given number, $t_{\max}$, terminate the process. Otherwise, set $t \leftarrow t+1$ and return to step 2.

In the early stage of this algorithm, nodes with a smaller n_i tend to be visited. As n_i increases, nodes with a large v_i are selected more intensively. This makes it possible to determine the optimal structure and geometry simultaneously.

C. *Hybridized parameter–topology optimization*

For the optimization of rotor geometry, PTO [3] is employed, where PO is applied to PMs, and TO is applied to the magnetic core.

First, the PO strategy is described. Here, $\boldsymbol{p}$ is the shape parameters of the PM shown in Fig. 2. Each PM configuration has different shape parameters. For an I-shaped PM, $\boldsymbol{p} = \{l, w, h\}$, length, width, and height. For a V-shaped PM, $\boldsymbol{p} = \{l, w, x_c, y_c, \theta_V\}$, length, width, center coordinates, and angle from the horizontal. For a U-shaped PM, $\boldsymbol{p} = \{R, \theta_U, w, h\}$, radius of curvature, angle of the arc, width, and height. A ∇-shaped magnet is represented by a combination of the parameters for I- and V-shaped PMs. If the number of PMs is doubled, the shape parameters are doubled to define each PM. For example, if "I-shaped" and "double" are selected in the selection part of the proposed method, optimization is performed with respect to $\boldsymbol{p} = \{l_1, w_1, h_1, l_2, w_2, h_2\}$, where the suffixes identify the PMs.

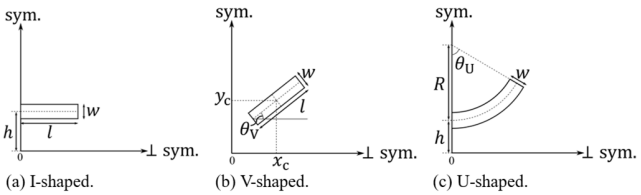

(a) I-shaped. (b) V-shaped. (c) U-shaped.

Fig. 2. Shape parameters for assumed PMs. "Sym." represents symmetric axis.

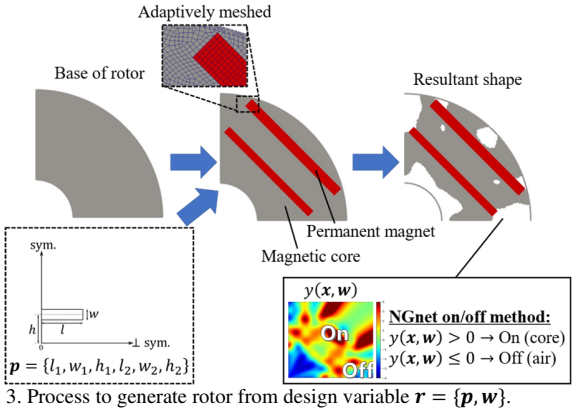

Fig. 3. Process to generate rotor from design variable $\boldsymbol{r} = \{\boldsymbol{p},\boldsymbol{w}\}$.

For TO of a magnetic core, the NGnet on/off method [1], [3] is adopted to parameterize the shape of the magnetic cores. In the NGnet on/off method, the material distribution is determined from the shape function $y(\boldsymbol{x},\boldsymbol{w})$ defined by

$$y(\boldsymbol{x},\boldsymbol{w}) = \sum_{i=1}^{N_G} w_i b_i(\boldsymbol{x}), \tag{4a}$$

$$b_i(\boldsymbol{x}) = \frac{\phi_i(\boldsymbol{x})}{\sum_{k=1}^{N_G}\phi_k(\boldsymbol{x})}, \tag{4b}$$

where $\boldsymbol{x}$, $\phi_i(\boldsymbol{x})$, $b_i(\boldsymbol{x})$, and N_G denote the position vector, Gaussian basis function uniformly arranged in the rotor region, normalized Gaussian function, and number of $\phi_i(\boldsymbol{x})$. If $y(\boldsymbol{x},\boldsymbol{w}) > 0$, the finite element (FE) with center $\boldsymbol{x}$ is set to magnetic material, and it is set to air otherwise. Here, $\boldsymbol{w} = \{w_i\}$ are the design parameters to be optimized.

Finally, PO and TO were performed simultaneously for the PTO at the leaf node. The set of design parameters $\boldsymbol{r} = \{\boldsymbol{p},\boldsymbol{w}\}$ is determined by dd-CMA-ES [8] in this study. During optimization, the rotor geometry was determined from $\boldsymbol{r}$, as shown in Fig. 3, which is analyzed by the FE method. After determining the PM geometry from $\boldsymbol{p}$, FE meshes were generated adaptively. The rotor geometry is determined by performing optimization with respect to $\boldsymbol{w}$ for the FE model represented by the generated mesh. This makes it possible to obtain fine FE meshes to represent PMs.

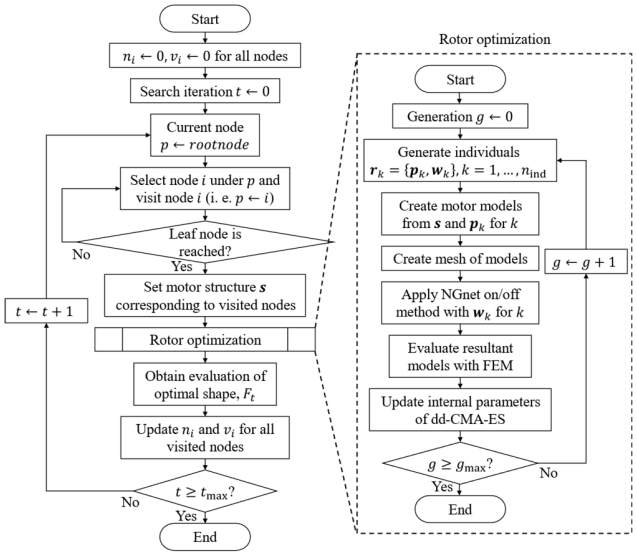

Fig. 4. Entire flowchart of proposed method.

D. *Flowchart of proposed method*

A flowchart of the proposed method is shown in Fig. 4. This algorithm consists of a tree search and rotor optimization, which can be implemented independently.

III. Numerical Results

A. *Optimization problem*

The proposed method with the tree structure shown in Fig. 1 was applied to the automatic design of a 24-slot PM motor. All models are based on the IEEJ Dmodel [1] [3] of four-pole and 24-slot PM motors. Fig. 5 shows the four-pole optimization model and Dmodel. The structure of the design region is determined by the PTO assuming symmetry. The two- and eight-pole optimization models had similar settings with an appropriate distribution of $\phi_i(\boldsymbol{x})$.

The optimization problem is defined as

$$F(\boldsymbol{s},\boldsymbol{r}) = 0.95\frac{T_{\text{avg}}}{T_{\text{avg}}^{\text{ref}}} - 0.05\frac{T_{\text{rip}}}{T_{\text{rip}}^{\text{ref}}} \rightarrow \max., \tag{5a}$$

$$\text{sub. to} \quad G_1(\boldsymbol{s},\boldsymbol{r}) = S^{\text{ref}} - S \geq 0, \tag{5b}$$

$$G_2(\boldsymbol{s},\boldsymbol{r}) = 0.05S - S_{\text{demag}} \geq 0, \tag{5c}$$

$$G_3(\boldsymbol{s},\boldsymbol{r}) = \min\left(\frac{S_1}{S_2}, \frac{S_2}{S_1}\right) - 0.5 \geq 0, \tag{5d}$$

where T_{avg} and T_{rip} denote the average torque and torque ripple, respectively, and $T_{\text{avg}}^{\text{ref}}$ and $T_{\text{rip}}^{\text{ref}}$ denote their reference values for Dmodel. Here, $T_{\text{rip}} = T_{\max} - T_{\min}$, where $T_{\max}$ and $T_{\min}$ are the maximum and minimum torques, respectively. The constraints are as follows: $G_1(\boldsymbol{s},\boldsymbol{r})$ is about the PM area S, which should be less than S^{ref} of Dmodel; $G_2(\boldsymbol{s},\boldsymbol{r})$ is relevant to the demagnetized area S_{demag}, which should be less than 5% of S; and $G_3(\boldsymbol{s},\boldsymbol{r})$ is applied only for doubled PMs or for ∇-shaped PMs, which prevents convergence to a single PM [9], where S_1 and S_2 denote the areas of the first and second PM (each pair of V-shaped PMs is considered to be one PM). One more constraint must be considered.

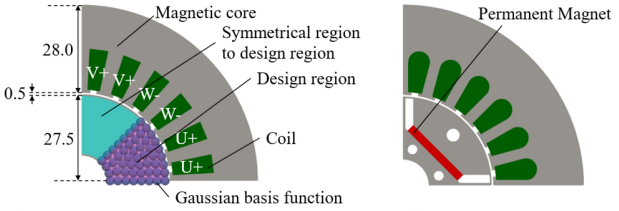

(a) Optimization model (four-pole) (b) IEEJ Dmodel (Referred as "Reference")

Fig. 5. Motor models used in this study (unit: mm). For Dmodel (b), current phase angle β is fixed to 30°.

TABLE I
Parameters for Machine and Optimization

Parameter	Value
Magnetic core sheet	50A400
Thickness (mm)	65.0
Current amplitude (A)	10.0
Number of turns of coil (turns)	35
Rotation speed (rpm)	1800
Residual flux density (T)	1.4
Number of design variables	53 (I-single), 55 (V-single), 54 (U-single), 58 (∇), 56 (I-double), 60 (V-double), 58 (U-double)
Number of individuals in rotor optimization, n_{ind}	64
Number of generations in rotor optimization, $g_{\max}$	300
Number of search iterations, $t_{\max}$	30

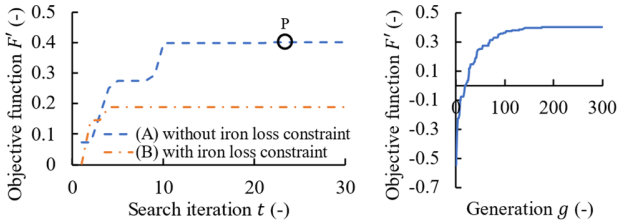

(a) Convergence history of tree search (b) Convergence history of rotor optimization, in case (A), $t = 22$.

Fig. 6. Convergence histories. At all the points in (a), rotor optimization is performed, whose convergence at point P is shown in (b).

$$\text{sub. to } G_4(\boldsymbol{s},\boldsymbol{r}) = P_{\text{iron}}^{\text{ref}} - P_{\text{iron}} \geq 0, \tag{5e}$$

where P_{iron} and $P_{\text{iron}}^{\text{ref}}$ denote the iron loss and that of Dmodel, respectively. In the following section, the results are compared for case (A) without considering the iron loss constraint $G_4(\boldsymbol{s},\boldsymbol{r})$ and for with (B) considering $G_4(\boldsymbol{s},\boldsymbol{r})$. The other settings are listed in Table I. The oracle penalty method [10] is employed to consider the constraints. In this method, $F(\boldsymbol{s},\boldsymbol{r})$ is converted to

$$F'(\boldsymbol{s},\boldsymbol{r}) = F(\boldsymbol{s},\boldsymbol{r}) - \Omega, \tag{6}$$

provided that $F(\boldsymbol{s},\boldsymbol{r}) > \Omega$ and all constraints are satisfied, where Ω is a constant that is set to 0.90, assuming $T_{\text{avg}} = T_{\text{avg}}^{\text{ref}}$ and $T_{\text{rip}} = T_{\text{rip}}^{\text{ref}}$. Otherwise, the penalty Ω is adaptively changed (for details, see a previous article [10]).

B. *Results*

Fig. 6 shows the convergence history of the tree search with and without constraint $G_4(\boldsymbol{s},\boldsymbol{r})$. In both cases, $F'(\boldsymbol{s},\boldsymbol{r})$

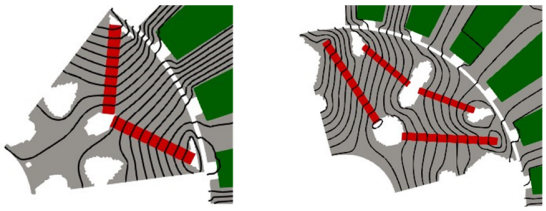

Case (A): Without iron loss constraint. $P_n = 8, \beta = 10°$, V-shaped, single.

Case (B): With iron loss constraint. $P_n = 4, \beta = 40°$, V-shaped, double.

Fig. 7. Optimized rotor shapes. Black lines represent flux lines.

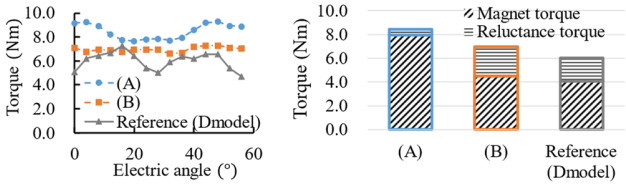

(a) Waveforms (b) Components

Fig. 8. Torque characteristics of optimized motors shown in Fig. 7.

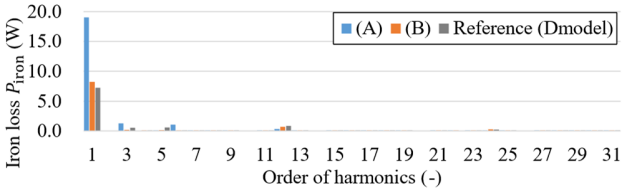

Fig. 9. Harmonics in iron loss for optimized motors shown in Fig.7.

converges well after 30 search iterations. Fig. 7 shows the resulting rotor structures. Figs. 8 and 9 show the torque characteristics and harmonics in the iron loss. For comparison, the values of Dmodel are also shown. These values are summarized in Table II. In case (A), an eight-pole motor is obtained with a V-shaped PM. The position and shape of the PM with flux barriers are optimized to enhance T_{avg}, mainly depending on the magnet torque. In contrast, in case (B), a four-pole motor is obtained with double V-shaped PMs with $\beta = 40°$. PMs and flux barriers form double layers in the rotor, which enhances T_{avg} by leveraging the reluctance torque. In both cases, T_{avg} increases and T_{rip} decreases compared with Dmodel. For iron loss, P_{iron} in case (A) is more than twice that of Dmodel. This is understandable since P_{iron} is not considered in case (A). The main reason for the higher value of P_{iron} in case (A) is that it has eight poles, so the electric angular speed

$$\omega_e = (P_n/2)\omega_m, \tag{7}$$

is higher than others. When P_{iron} is considered in case (B), the optimal shape has almost the same P_{iron} as that of Dmodel, which means that the constraint is satisfied.

Table III shows the number of visits at the first level of the tree and the number of poles in each case. In case (A), four- and eight-pole nodes are mainly visited. In case (B), a four-pole node is visited more intensively, mainly for the above-mentioned reasons. In both cases, the two-pole node is not visited frequently, which implies that it has less potential to generate a high T_{avg}.

For verification, a conventional PTO in which the rotor geometry was performed while the motor structure was fixed to Dmodel. The values in parentheses in Table II show the results. The proposed method yields higher values of $F'(\boldsymbol{s}, \boldsymbol{r})$ compared with the conventional PTO, whereas all the constraints are satisfied in all cases. This demonstrates the effectiveness of the proposed method. The tree structure can be modified to consider other characteristics. The proposed method provides a general framework for the automatic design of electric motors and other devices.

TABLE II
CHARACTERISTICS FOR MOTOR MODELS OBTAINED IN EACH CASE

Case	$F'(\boldsymbol{s}, \boldsymbol{r})$	T_{avg} (Nm)	T_{rip} (Nm)	S (mm^2)	S_{demag} (mm^2)	P_{iron} (W)
Case (A)	0.401 (0.349)	8.42 (8.05)	1.62 (1.23)	218 (218)	8.60 (3.30)	22.0 (17.8)
Case (B)	0.188 (0.171)	6.97 (6.84)	0.682 (0.507)	217 (217)	7.84 (9.63)	9.69 (9.69)
Reference	0.00	6.02	2.61	218	0.00	9.71

The values (.) represent the characteristics of motors obtained by PTO, where the basic motor structures are fixed to those of Dmodel: $P_n = 4$, $\beta = 30°$, I-shaped, and single. The other settings are the same as those in Table I.

TABLE III
NUMBER OF VISITS FOR NUMBER OF POLES IN EACH CASE

Case	2-pole	4-pole	8-pole
Case (A)	4	15	11
Case (B)	7	17	6

IV. CONCLUSION

A novel automatic design method was proposed that optimizes the basic motor structure as well as the rotor geometry. Its validity was demonstrated for the optimization of PM motors. It can be easily extended to other motors and devices.

REFERENCES

[1] T. Sato, K. Watanabe, and H. Igarashi, "Multimaterial Topology Optimization of Electric Machines Based on Normalized Gaussian Network," *IEEE Trans. Magn.*, vol. 51, no. 3, Art. no. 7202604, 2015.

[2] Y. Yamashita and Y. Okamoto, "Design Optimization of Synchronous Reluctance Motor for Reducing Iron Loss and Improving Torque Characteristics Using Topology Optimization Based on the Level-Set Method," *IEEE Trans. Magn.*, vol. 56, no. 3, Art no. 7510704, 2020.

[3] S. Hiruma, M. Ohtani, S. Soma, Y. Kubota, and H. Igarashi, "Novel Hybridization of Parameter and Topology Optimizations: Application to Permanent Magnet Motor," *IEEE Trans. Magn.,* vol. 57, no. 7, Art no. 8204604, 2021.

[4] T. Sato and M. Fujita, "A Data-Driven Automatic Design Method for Electric Machines Based on Reinforcement Learning and Evolutionary Optimization," *IEEE Access*, vol. 9, pp. 71284–71294, 2021.

[5] D. Silver *et al.*, "A general reinforcement learning algorithm that masters chess, shogi, and Go through self-play," *Science,* vol. 362, no. 6419, pp.1140–1144, 2018.

[6] A. Khan, C. Midha and D. A. Lowther, "Sequence-Based Environment for Topology Optimization," *IEEE Trans. Magn.*, vol. 56, no. 3, Art no. 7510904, 2020.

[7] M. Guillaume, J.-B. Chaslot, M. H. M. Winands, H. Jaap Van Den Herik, and J. W. H. M. Uiterwijk, "Progressive Strategies for Monte-Carlo Tree Search," *New Math. And Nat.*, vol. 4, no. 3, pp. 343–357, 2008.

[8] Y. Akimoto and N. Hansen, "Diagonal Acceleration for Covariance Matrix Adaptation Evolution Strategies," *Evol. Comput.*, vol. 28, no. 3, pp. 405–435, 2019.

[9] Y. Otomo, private communication.

[10] M. Schlüter and M. Gerdts, "The oracle penalty method," *J. Glob. Opt.*, vol. 47 no. 2, pp. 293–325, 2010.